THE JOURNAL OF PHYSICAL CHEMISTRY C

Article

Cite This: J. Phys. Chem. C 2019, 123, 7054−7060

pubs.acs.org/JPCC

Chemical Potential of Nitrogen at High Pressure and High Temperature: Application to Nitrogen and Nitrogen-Rich Phase Diagram Calculations

Hanof Alkhaldi and Peter Kroll*

Department of Chemistry and Biochemistry, The University of Texas at Arlington, 700 Planetarium Place, Arlington, Texas 76019, United States

ABSTRACT: The chemical potential change of nitrogen at high pressure/high temperature is a crucial ingredient for predicting the formation of nitrogen-rich compounds. Here, we provide intelligible data for the chemical potential change of molecular nitrogen at temperature and pressure conditions relevant for experiments in the diamond anvil cell. In combination with first-principles calculations, we derive pressure−temperature phase diagrams readily accessible to guide experimental efforts. We show the validity of our approach for three characteristic systems: pure nitrogen and nitrogen-rich Si−N and Ti−N phases appearing at high pressure/high temperature.

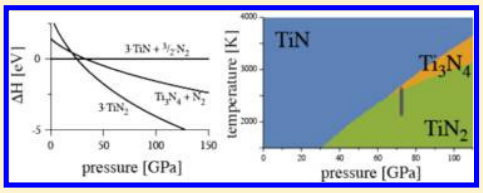

INTRODUCTION

High-pressure (h-p) nitrogen chemistry has seen tremendous advances over the last 3 decades thanks to diligent experimental work. The pursuit of super-hard and high energy density materials has driven many endeavors, and several new nitrogen-rich compounds have been synthesized.[1−13] With the advent of accurate density functional calculations, it became possible to predict new phases and the range of pressure they will emerge.[1,14,15] The availability of massive high-performance computers today makes high-throughput searches, employing a variety of structure search algorithms feasible, and even more compound systems involving nitrogen are explored.[16−21]

In a recent comprehensive work, Sun et al. identified stable and metastable nitrogen-rich compounds and analyzed their enthalpy of formation from the elements.[20] Their work highlights the importance of the chemical potential of nitrogen for the successful synthesis of nitrogen-containing compounds. Evidently, molar enthalpy equals chemical potential in the pure state only at absolute zero. Elevated temperature and pressure as well as the chemical environment, however, yield substantial differences between the two.[22]

Our focus is the chemical potential of nitrogen at high-pressure/high-temperature conditions (h-p/h-T) above 5 GPa and from 1500 to 4000 K. These conditions are characteristic for laser-heated experiments carried out in the diamond anvil cell (DAC), where a synthesis of nitrogen-rich compounds may occur via direct synthesis from the elements.[1,3] Even if fluid molecular nitrogen is not used as a pressure medium, it may evolve from reactants during heating and has to be accounted for in a reaction mixture. Standard textbook approaches relate the chemical potential change of nitrogen at h-p/h-T to its fugacity, which can adopt astronomical values even at experimentally accessible pressure.[23] We have previously described estimates for the fugacity of molecular nitrogen for h-p/h-T.[24] Here, we provide intelligible data for the chemical potential change of molecular nitrogen at temperature and pressure conditions relevant for experiments in the DAC. We then combine the thermochemical data with first-principles calculations into thermodynamic calculations of pressure−temperature phase diagrams. We consider three characteristic compound systems, N, Si−N, and Ti−N, to highlight the difference between estimates of phase stability based on enthalpy alone and predictions involving the impact of chemical potential changes at h-p/h-T conditions and to show the validity of our approach.

COMPUTATIONAL METHOD

First-Principles Calculations. Calculations of total energy and volume are done within density functional theory, as implemented in Vienna abs initio simulation package.[25−28] We use the strongly constrained and appropriately normed (SCAN) functional[29] together with the projector-augmented wave method.[30,31] Consistency checks have been done with the generalized gradient approximation (GGA-Perdew−Burke-Ernzerhof (PBE)) as well.[32,33] All results are obtained using a plane wave cutoff energy of 500 eV with forces converged to better than 1 meV/Å. The Brillouin zone of each structure is sampled by k-point meshes with grid sizes smaller than 0.03 Å^{-1}. With the parameters above, enthalpy differences between structures are converged to better than 1 meV.

For every structure, we compute energy E as a function of volume V, reducing V stepwise to simulate higher densities and pressures. The resulting $E-V$ data yields pressure p by numerical differentiation, $p = -\partial E/\partial V$, and enthalpy $H = E + pV$. Reaction enthalpies ΔH as a function of pressure at zero temperature are computed based on enthalpies of products and

Received: January 16, 2019
Revised: March 3, 2019
Published: March 19, 2019

DOI: 10.1021/acs.jpcc.9b00476
J. Phys. Chem. C 2019, 123, 7054−7060

Table 1. Changes of Chemical Potential, $\Delta\mu(T, p_{N_2})$ (in eV/Atom), of Nitrogen, Treating Nitrogen as Perfect Gas, $\gamma = 1$ ($\ln\gamma = 0$)

$\Delta\mu(T, p_{N_2})$	20 GPa	40 GPa	60 GPa	80 GPa	100 GPa	120 GPa	140 GPa
1500 K	−0.89	−0.85	−0.82	−0.80	−0.79	−0.78	−0.77
2000 K	−1.27	−1.21	−1.18	−1.15	−1.13	−1.12	−1.10
2500 K	−1.67	−1.60	−1.55	−1.52	−1.50	−1.48	−1.46
3000 K	−2.09	−2.00	−1.95	−1.91	−1.88	−1.86	−1.84

Table 2. Changes of Chemical Potential, $\Delta\mu(T, p_{N_2})$ (in eV/Atom), of Nitrogen, with Fugacity Approximated Using the Moderate Extrapolation, eq f1

$\Delta\mu(T, p_{N_2})$	20 GPa	40 GPa	60 GPa	80 GPa	100 GPa	120 GPa	140 GPa
1500 K	−0.21	−0.16	−0.13	−0.11	−0.10	−0.08	−0.07
2000 K	−0.61	−0.54	−0.51	−0.48	−0.46	−0.45	−0.44
2500 K	−1.02	−0.94	−0.90	−0.87	−0.84	−0.82	−0.81
3000 K	−1.45	−1.36	−1.31	−1.27	−1.24	−1.22	−1.20

reactants. This data is commonly used to identify the convex hull of a phase system. Neglecting further impact of temperature and entropy differences, reaction Gibbs energies $\Delta G = \Delta H - T\Delta S$ are approximated by ΔH. Locating $\Delta H = 0$ then yields an estimate of transition pressures. These estimates are excellent guidelines predicting solid-state reactions at constant composition, not at least because entropy differences that contribute to reaction Gibbs energies ΔG for solid-state reactions are usually small in comparison to changes of ΔH within a few GPa of pressure.

Once a gaseous or fluid reactant or product is involved, however, effects of entropy must be included. This is imperative for reactions involving pure nitrogen, which is why a consideration of the chemical potential μ of nitrogen, its Gibbs molar energy, and its increment relative to molar enthalpy is important.[15,20,24]

Thermodynamic Calculations. The chemical potential of nitrogen gas $\mu(T, p_{N_2})$ depends on temperature T and nitrogen partial pressure p_{N_2} via

$$\mu(T, p_{N_2}) = \mu(T, p_0) + kT \ln\left(\frac{f}{p_0}\right) = \mu(T, p_0) + kT \ln\left(\frac{\gamma p_{N_2}}{p_0}\right) = \mu(T, p_0) + kT \ln\left(\frac{p_{N_2}}{p_0}\right) + kT \ln\gamma$$

Herein, f is the fugacity of nitrogen, p_0 is a reference nitrogen partial pressure for which we choose 1 bar (0.1 MPa), and k is the Boltzmann constant. The second equality relates fugacity f to nitrogen partial pressure p_{N_2} and introduces the fugacity coefficient γ. For a perfect gas, $f = p_{N_2}$ and $\gamma = 1$ hold. The last term in the equation, $kT \ln\gamma$, then shows the impact of a deviation from perfect gas behavior on the chemical potential. To provide examples: $\ln\gamma = 20$, thus $f \approx 10^9 p_{N_2}$ describes the experimental data of nitrogen at 300 K and 2 GPa, whereas at 2000 K and 2 GPa, $\ln\gamma = 2.3$.[23,34]

There is currently no rigorous theoretical framework available to assess the fugacity of nitrogen at elevated temperatures and pressures for different chemical environments. However, changes of the nitrogen chemical potential above the boiling point at an ambient pressure, $\Delta\mu(T, p_{N_2})$, have been well documented in thermochemical tables.[22] Since changes of μ in the gaseous state dominate those in the solid and liquid states by far, it is justified to neglect the increment of μ from absolute zero up to the boiling point and approximate the chemical potential at these conditions simply by enthalpy H of a solid molecular phase of nitrogen. We thus receive

$$\mu(T, p_{N_2}) \approx H(p_{N_2}) + \Delta\mu(T, p_{N_2})$$

and the chemical potential increment $\Delta\mu(T, p_{N_2})$ is given by

$$\Delta\mu(T, p_{N_2}) = \Delta\mu(T, p_0) + kT \ln\left(\frac{p_{N_2}}{p_0}\right) + kT \ln\gamma$$

The first term in this equation reflects the tabulated thermochemical data, whereas the second term describes the dependence of the chemical potential of a perfect gas on pressure. The third term accounts for all deviations from perfect behavior, collected in the fugacity. For a perfect gas, $\gamma = 1$, thus $\ln\gamma = 0$, and the third term vanishes. In general, fugacity γ will depend on all parameters of a system but especially on the partial pressure of the gas and on temperature.

In the previous work, we provided three different approaches to account for $\Delta\mu(T, p_{N_2})$ at high temperatures and high pressures. A first approach assumes perfect gas behavior, thus $\ln\gamma = 0$.[15,35] A second proposal follows a moderate extrapolation of experimental data[24]

$$\ln\gamma = \alpha(T)[1 - \exp(-\beta(T)p_{N_2})] \quad \text{(f1)}$$

with $\alpha(T) = \alpha_1/T + \alpha_2/T^2 + \alpha_3/T^3$ and $\beta(T) = \beta_0 + \beta_1/T + \beta_2/T^2$.

Coefficients are: $\alpha_1 = 14.0707$, $\alpha_2 = 2.40815$, $\alpha_3 = 0.86685$, $\beta_0 = 0.29775$, $\beta_1 = 0.09503$, $\beta_2 = 0.00996$. A third estimate of γ extrapolates experimental data in a more progressive way[24]

$$\ln\gamma = \alpha/T \ln(1 + \beta p_{N_2}) \quad \text{(f2)}$$

with $\alpha = 10.4583$ and $\beta = 0.3879$. In both extrapolation formulas, the temperature T is given in units of 1000 K and the pressure p_{N_2} in GPa. For convenience, we provide data of $\Delta\mu(T, p_{N_2})$ based on these approaches for conditions relevant to high-pressure/high-temperature syntheses of nitride compounds shown in Tables 1−3.

DOI: 10.1021/acs.jpcc.9b00476
J. Phys. Chem. C 2019, 123, 7054−7060

Table 3. Changes of Chemical Potential, $\Delta\mu(T, p_{N_2})$ (in eV/Atom), of Nitrogen, with Fugacity Approximated Using the Progressive Extrapolation, eq f2

$\Delta\mu(T, p_{N_2})$	20 GPa	40 GPa	60 GPa	80 GPa	100 GPa	120 GPa	140 GPa
1500 K	0.09	0.42	0.62	0.76	0.87	0.96	1.04
2000 K	−0.29	0.05	0.26	0.41	0.53	0.63	0.71
2500 K	−0.69	−0.33	−0.12	0.04	0.16	0.26	0.35
3000 K	−1.11	−0.74	−0.51	−0.35	−0.22	−0.12	−0.03

Using thermodynamic data together with the various extrapolation formulas, it is now straightforward to compute the chemical potential $\mu(T, p_{N_2})$ of nitrogen at high temperatures and high pressures. Assuming, furthermore, that the increment $\Delta\mu(T, p_{N_2})$ dominate all further temperature effects, especially the entropy differences between solid-state products and reactants, we can combine the thermodynamic calculations with first-principles calculations of enthalpy and compute reaction Gibbs energies ΔG. Locating equilibrium lines and identifying the most stable system at a given temperature and pressure, finally, result in temperature−pressure phase diagrams.

RESULTS

On the Nitrogen Phase Diagram. We first apply the approach combining first-principles computations with thermodynamic calculations to identify the phase boundary between molecular nitrogen and polymeric nitrogen. Triple-bonded molecular nitrogen is represented using the crystal structure of ε-N_2 (SpGr. $R\bar{3}c$ (167), Z = 16). Choosing α-N_2 (SpGr. $Pa\bar{3}$ (205), Z = 8) instead provides equivalent enthalpy−pressure data if a pressure-induced distortion of the cubic into an orthorhombic (*Cmca*) structure is allowed. Both ε- and α-phases remain "molecular", comprising isolated N_2 molecules of up to about 200 GPa, when they "polymerize" spontaneously. Single-bonded polymeric nitrogen, also termed cubic-gauche phase, cg-N, adopts a cubic structure (SpGr. $I2_13$ (199), Z = 8).

At experimental conditions, cg-N emerges at pressures above 110 GPa and temperatures above 2000 K.[4] Additional experiments report the formation of transparent cg-N at 120−130 GPa above 2000 K,[36] at 165 GPa in excess of 2000 K,[37] and at 140 GPa when heating above 1450 K. All reports agree that the formation of cg-N at high-pressure high-temperature conditions is a complex kinetic process passing through multiple intermediates. Longer heating enhances the phase content of polymeric nitrogen, whereas heating at higher temperatures accelerates its formation.

Calculating the energy−volume (E−V) data for molecular and polymeric nitrogen and deriving the corresponding ΔH−p diagram (Figure 1) yield a transition pressure p_t for the transformation between the two phases of 59.3 GPa (53.3 GPa using PBE). This is in line with previous reports of computed values of p_t[14,38] but obviously not corresponding to the experimental conditions listed above. At 110 GPa, the lowest reported transition pressure, the enthalpy difference between ε-N_2 and cg-N is 0.48 eV/atom (0.55 eV/atom using PBE), clearly favoring the polymeric form of nitrogen. Assuming that the experimental conditions (110 GPa, 2000 K) reflect the equilibrium between molecular N_2 and cg-N, the chemical potential of both phases is equal at these conditions.

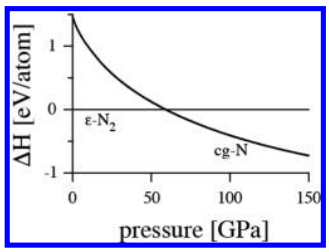

Figure 1. Enthalpy−pressure (ΔH−p) of polymeric-N relative to molecular ε-N_2 computed using the SCAN functional. The enthalpy difference ΔH is given in eV per atom.

Consequently, the computed enthalpy for molecular nitrogen is augmented by an increment of −0.48 eV/atom (negative relative to cg-N) to yield its chemical potential. Therefore, $\Delta\mu$(2000 K, 110 GPa) = −0.48 eV/atom. This value of $\Delta\mu$ is in agreement with the data derived using the moderate extrapolation of fugacity, Table 2. The more progressive estimate may not be ruled out, since many times, temperatures have been described as "in excess of 2000 K". Consequently, experimental data for the synthesis of cg-N supports our proposal that the two extrapolations can be regarded as lower and upper boundaries for the fugacity of nitrogen at high pressures.

We now combine for molecular nitrogen the first-principles calculations of enthalpy as a function of pressure with the thermodynamic calculations of chemical potential changes as a function of temperature and pressure. On the other side, Gibbs energy of the solid cubic-gauche phase of nitrogen is approximated by its enthalpy. This approach neglects contribution by vibrational entropy and further effects. However, this error occurs on both sides of the equilibrium equation and will, to a large extent, cancel out. Besides, these contributions are dwarfed by the chemical potential change for molecular nitrogen (and by its uncertainty). We acknowledge that the dominant error in these calculations is within the estimate of $\Delta\mu(T, p_{N_2})$, and more experiments will be helpful to yield more accurate estimates of $\Delta\mu(T, p_{N_2})$. The phase boundary between molecular nitrogen and the phase of cg-N is then located by equating the Gibbs energies of the two phases, and the results are shown in Figure 2. Obviously, the experimental results—the phase boundary between molecular and polymeric nitrogen—are well characterized through either the moderate or progressive extrapolation of fugacity for molecular nitrogen. Treating nitrogen as a perfect gas does not yield a thermodynamically stable cg-N at 110 GPa and 2000 K, whereas the two extrapolating approximations do.

On the Silicon−Nitrogen Phase Diagram. We apply the computational approach next to the Si−N phase system, focusing on the surprising synthesis of SiN_2. Until 1999, α- and β-Si_3N_4 were the only known crystalline ambient pressure modifications of silicon nitride. Zerr et al. then synthesized a spinel-type γ-Si_3N_4 (SpGr. $Fd\bar{3}m$ (227), Z = 8) by reacting silicon and molecular nitrogen at 15 GPa and 2000 K.[1] A postspinel modification δ-Si_3N_4 was later been predicted to adopt a $CaTi_2O_4$-type structure and succeed γ-Si_3N_4 above 160 GPa.[39] SiN_2 with a pyrite-type structure (SpGr. $Pa\bar{3}$ (205), Z = 4) comprising the pernitride N_2^{4-}-anion was first considered by Weihrich et al.[40] In 2014, Chen et al. computed the pyrite-type SiN_2 to be enthalpically favored over a combination of γ-Si_3N_4 and N_2 at pressures above 17 GPa.[41] Subsequently, this

DOI: 10.1021/acs.jpcc.9b00476
J. Phys. Chem. C 2019, 123, 7054−7060

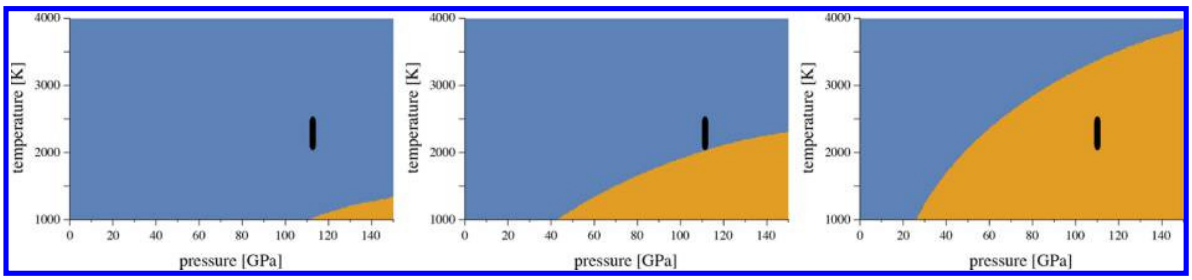

Figure 2. Pressure−temperature phase diagram of nitrogen showing the phase boundary between molecular (ε-N_2) and polymeric (cg-N) nitrogen based on a combination of first-principles (SCAN functional) and thermodynamic calculations. For the fugacity of nitrogen, we use (left) the perfect gas approximation, (middle) the moderate, and (right) the progressive extrapolation formula. The thick line in each diagram indicates reported experimental conditions from ref 4 for the formation of polymeric nitrogen.

phase was obtained through direct synthesis from the elements using laser heating at approximately 60 GPa.[42] Unfortunately, no estimate of the temperature during the synthesis of SiN_2 has been given. Notably, applying only 50 GPa of pressure but the same temperature conditions yields only γ-Si_3N_4 and not SiN_2, indicating a boundary between the two phases. At this point, it is possible to think of Si−N phases with even higher nitrogen content. As one example, we consider SiN_4 with a structure related to the calcite type of $CaCO_3$ (SpGr. $R\bar{3}c$ (167), $Z = 6$). At 71 GPa (62 GPa in PBE), this candidate type of SiN_4 will become more favorable by enthalpy relative to SiN_2 and molecular nitrogen, see Figure 3. In other words, it will appear on the convex hull of the Si−N phase system between SiN_2 and N.

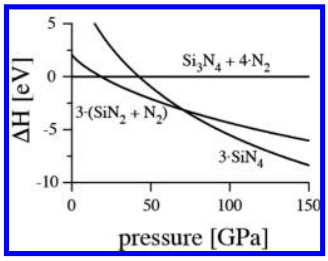

Figure 3. Relative enthalpy−pressure (ΔH−p) diagram comparing Si_3N_4 + $4N_2$, $3(SiN_2 + N_2)$, and $3SiN_4$ computed using the SCAN functional. Enthalpy is given relative to γ-Si_3N_4 and molecular ε-N_2.

As in the nitrogen phase system, we note a discrepancy between computed and observed phase boundaries between γ-Si_3N_4 and SiN_2. Once again, we can relate the significant shift in transition pressure to the chemical potential increment of molecular nitrogen involved in the phase change. According to Figure 3, the enthalpy difference between $3SiN_2$ and γ-Si_3N_4 + N_2 at 60 GPa is 2.6 eV (2.9 eV in PBE). Assuming that both phases are in equilibrium, this implies that at experimental conditions, where the pressure refers to the partial pressure of nitrogen, p_{N_2}, the chemical potential of nitrogen is 1.3 eV per N atom lower than its computed enthalpy. Therefore, $\Delta\mu(T_{syn}, 60\ \text{GPa}) = -1.3$ eV/atom. It is justified to expect that the temperature of synthesis T_{syn} exceeds 2000 K in these experiments.[1] Inspecting the values of $\Delta\mu$ at 60 GPa in Tables 1−3, we find corresponding data, for example, using perfect gas data (~2300 K) or the moderate extrapolation of fugacity of nitrogen (~3000 K). As to the likelihood of SiN_4 emerging at high nitrogen pressure, Figure 3 yields that the enthalpy difference between SiN_2 + N_2 and SiN_4 at 100 GPa is $1/3 \times 1.15$ eV = 0.38 eV. Thus, we expect the formation of SiN_4 only if the chemical potential increment $\Delta\mu$ is larger than −0.19 eV. Assuming the moderate extrapolation formula to be valid, this can only happen below 1600 K at 100 GPa. Note that above 110 GPa the formation of cg-N is observed.

Combining first-principles and thermodynamic calculations, we derive the phase diagrams collectively shown in Figure 4. Focusing on a pressure of 60 GPa, we find that the moderate extrapolation formula for the fugacity of nitrogen yields fitting result if we assume typical temperatures between 2000 and 3000 K in such a laser-heating experiment.[1] Even if we treat nitrogen as a perfect gas, a pernitride SiN_2 has a small range of stability above 2000 K at 60 GPa before being decomposed into Si_3N_4 and nitrogen at higher temperatures. A reduced fugacity of nitrogen would also describe the formation of γ-

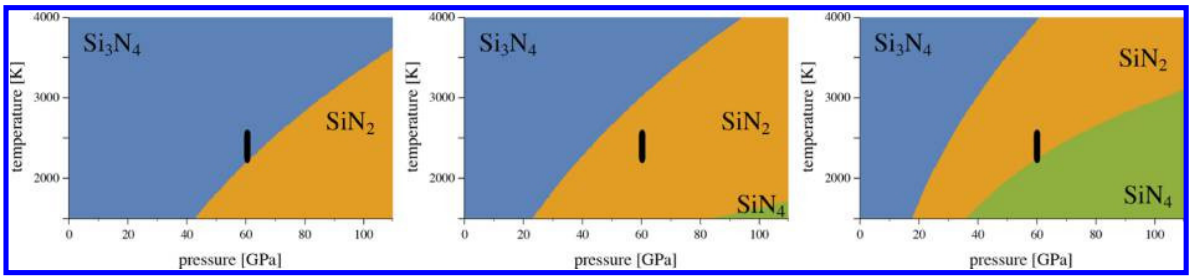

Figure 4. Temperature−pressure phase diagrams for the silicon−nitrogen system involving Si_3N_4, SiN_2, and SiN_4. Pressure refers to nitrogen partial pressure, p_{N_2}. For the fugacity of nitrogen, we use the (left) perfect gas approximation, (middle) the moderate, and (right) the progressive extrapolation formula. The thick line in each diagram indicates the pressure (60 GPa) for the formation of SiN_2 reported in ref 42 together with a good-faith estimate of the temperature of synthesis. The transition from α/β-Si_3N_4 to γ-Si_3N_4 occurring at about 15 GPa had been omitted from the diagrams.

DOI: 10.1021/acs.jpcc.9b00476
J. Phys. Chem. C 2019, 123, 7054−7060

Si_3N_4 at 50 GPa from the elements. Based on the more moderate approximation of fugacity, the synthesis of SiN_4 will require pressures at about 100 GPa and may eventually be impossible due to the appearance of cg-N. Indeed, we find that SiN_4 is less favorable by enthalpy than SiN_2 and cg-N at any pressure.

On the Titanium−Nitrogen Phase Diagram. Our third application of combining first-principles and thermodynamic calculations addresses the nitrogen-rich part of the titanium−nitrogen phase diagram. A first account of the Ti−N phase diagram involving rock salt TiN (SpGr. $Fm\bar{3}m$ (225), $Z = 4$) and Th_3P_4-type Ti_3N_4 (SpGr. $I\bar{4}3d$ (220), $Z = 4$), while treating nitrogen as a perfect gas, located the phase boundary between TiN and Ti_3N_4 of 75 and 100 GPa, at 2000 and 2800 K, respectively.[15,35] Subsequent structure searches discovered a pernitride TiN_2 (SpGr. $I4/mcm$ (140), $Z = 4$) to appear on the convex hull for pressures above 26.6 GPa, surpassing Ti_3N_4 at any higher pressure.[17] Experimental studies first reported the synthesis of TiN_2 at 73 GPa and 2300 K.[43] Subsequently, a similar experiment (75 GPa, 2400 K) produced the long-sought Th_3P_4-type Ti_3N_4.[44] Careful analysis of both experiments indicates that pernitride TiN_2 and Th_3P_4-type Ti_3N_4 were produced each time at different locations of the reaction chambers.[44]

Computing energies and enthalpies for the three systems $3TiN + 3/2N_2$, $Ti_3N_4 + N_2$, and $3TiN_2$ yields the enthalpy−pressure diagram of Figure 5, left. We find that below 24.6 GPa

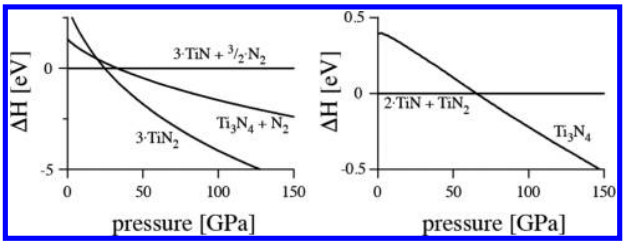

Figure 5. (Left) Relative enthalpy−pressure (ΔH−p) diagram comparing $3TiN + 3/2N_2$, $Ti_3N_4 + N_2$, and $3TiN_2$ computed using the SCAN functional. Enthalpy is given relative to TiN and molecular ε-N_2. (Right) Enthalpy of reaction for $2TiN + TiN_2 \rightarrow Ti_3N_4$. Enthalpy is given per formula unit Ti_3N_4.

the $TiN + 1/2N_2$ system is favored by enthalpy, whereas above this pressure, TiN_2 is the most favorable compound. As to the question whether Ti_3N_4 may appear[44] or may not appear[17] on the convex hull, we find the reaction $2TiN + TiN_2 \rightarrow Ti_3N_4$ to be exothermic above 65.4 GPa (Figure 5, right). Thus, Ti_3N_4 appears on the convex hull between TiN and TiN_2—but how will this relate to thermodynamical stability at elevated temperatures?

The results of phase diagram calculations are shown in Figure 6. A common feature is the small wedge of the stability field of Ti_3N_4 between the much larger regions corresponding to TiN and TiN_2. The wedge starts at about 62 GPa and emerges at quite different temperatures depending on the approximation for the fugacity of nitrogen. However, in each approximation, it widens its range with increasing pressure. At 75 GPa, its width is 200 K and enlarges to 500 K at 110 GPa. With respect to experimental condition, 75 GPa and 2400 K, it appears that the moderate approximation to the fugacity of nitrogen predicts best the outcome of the experiment. Temperature conditions in the diamond anvil cell are not equal throughout the chamber, and large variations can appear. Thus, an apparent "coexistence" of Ti_3N_4 and TiN_2 is likely related to different temperature conditions, with each phase being synthesized at its thermodynamical stable conditions before being quenched rapidly.

DISCUSSION

Predicting the chemical synthesis of new high-pressure nitride phases from their elements in standard laser-heated diamond anvil experiments requires the consideration of reaction equilibria of nitride compounds with molecular nitrogen—as a function of pressure and temperature. Considering a "convex hull" of relative enthalpy involving nitrogen may serve as an initial guideline, but the substantial decrease of the chemical potential of nitrogen above the boiling point (in the range of −1.5 to −3.5 eV per N atom for 1500−3000 K, respectively[22]) limits its predictive value. At higher pressure, this effect is countered, and experimental data suggests that nitrogen becomes extremely active as expressed through its fugacity.

Comparing experimental data for the synthesis of cg-N with the computed phase diagrams of Figure 2 undoubtedly supports a significant change of chemical potential as well as a substantial magnitude of the fugacity of nitrogen at an elevated pressure and temperature. For the pure system, the extrapolation formulas (eqs f1 and f2) provide lower and upper boundaries for the fugacity of nitrogen at high pressures and temperatures. Analysis of computed Si−N and Ti−N phase diagrams and the available experimental data corroborate the notion that the moderate approach to fugacity (eq f1) carries a higher weight. The case of simultaneous synthesis of Ti_3N_4 and TiN_2 shows the delicacy of the approach. Indeed, at 75 GPa, Ti_3N_4 has only a small temperature stability window ($\Delta T \approx$

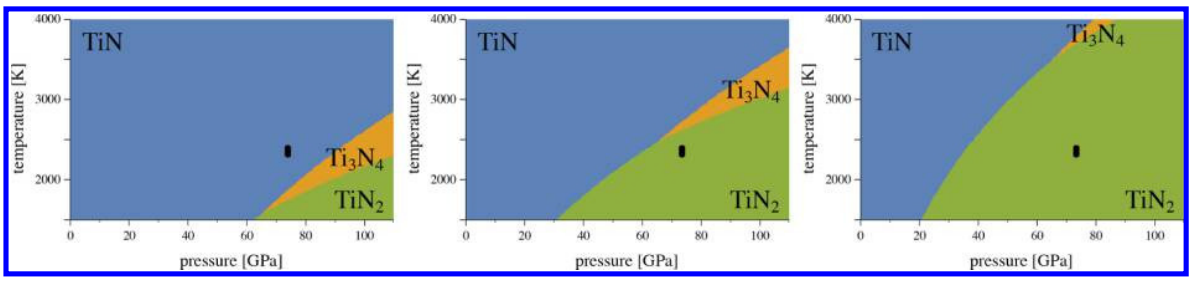

Figure 6. Temperature−pressure phase diagrams for the titanium−nitrogen system involving TiN, Ti_3N_4, and TiN_2. Pressure refers to nitrogen partial pressure, p_{N_2}. For the fugacity of nitrogen, we use the (left) perfect gas approximation, (middle) the moderate, and (right) the progressive extrapolation formula. The thick line in each diagram indicates the experimental conditions for the formation of Ti_3N_4 and TiN_2 reported in refs 43 and 44.

DOI: 10.1021/acs.jpcc.9b00476
J. Phys. Chem. C 2019, 123, 7054−7060

200 K) available for its synthesis, and this condition was hit at some spots in the experiment.

Additional support stems from the synthesis of RuN_2. Early predictions located the phase boundary between 25 and 40 GPa at temperatures between 2000 and 3000 K, respectively.[45] RuN_2 was then synthesized at pressures above 32 GPa, and while no temperature measurements were made, there was an indication that the temperature exceeded 2000 K.[46] Up to 20 GPa, even the treatment of nitrogen as perfect gas can yield reasonable estimates of phase boundaries at high temperature.[15,35]

The major source of error in our phase diagram calculations originates from limited knowledge about the fugacity of nitrogen. Note that for high-pressure nitrides, typical contributions of vibrational entropy differences to ΔG remain very small. At 2000 K, these contributions are well below 0.1 eV/atom.[19,47] Configurational entropy caused by defects or via mixing may in principle contribute up to 0.1 eV at 2000 K per active site if we assume ideal mixing. In most compound systems, such contributions are compensated by a few GPa of pressure change. In comparison, the uncertainty in chemical potential change is larger, and taking the moderate extrapolation formula as a base, we estimate a margin of ±0.2 eV per nitrogen atom. To evaluate how such an error propagates into pressure or temperature imprecisions, one can plot the convex hull for a particular temperature or make plots of relative Gibbs energy (ΔG) at a certain temperature as a function of pressure. Likewise, it is possible to plot ΔG for a given pressure as a function of temperature. These "slices" through the computed phase diagram will also help to identify phases, which are closely above the minimum Gibbs energy system.

Of course, the combination of first-principles and thermodynamic calculations requires the input of good structure candidates, making the various methods of structure searches indispensable for the exploration of new materials.[17,20] Together with the method we deliver, they provide a comprehensive tool to guide the synthesis of nitrogen-rich compounds at high pressure and high temperature. Chemical potential of nitrogen at high pressure and high temperature is also required for the discussion of defect chemistry in nitride compounds.[48] Further implications of our quantitative approach are for earth and planetary science, where the incorporation of nitrogen in silicate glasses and minerals is studied and its evolution in planetary bodies is discussed.[49]

Last, we note that we have chosen simple extrapolation formulas and only consider the impact of nitrogen partial pressure and temperature on fugacity. Further experimental pressure and temperature data are needed to provide better estimates for fugacity and chemical potential change of nitrogen at high-pressure high-temperature conditions in different chemical environments.

CONCLUSIONS

We provide a pathway to compute pressure−temperature phase diagrams of nitrogen-rich compounds, combining experimental thermochemical data with first-principles calculations. The approach is validated by comparison to experimental data for the synthesis of polymeric nitrogen, the phase boundary between silicon nitride and silicon pernitride, and the appearance of three nitrogen-rich Ti−N phases within a small pressure−temperature range. Overall, we deliver a rational strategy to predict temperature−pressure conditions for the synthesis of nitrogen-rich compounds. High-pressure researchers can apply the approach to identify new nitrogen-rich materials attainable via direct synthesis from the elements.

AUTHOR INFORMATION

Corresponding Author

*E-mail: pkroll@uta.edu.

ORCID

Hanof Alkhaldi: 0000-0002-6478-1438

Peter Kroll: 0000-0003-4782-2805

Notes

The authors declare no competing financial interest.

ACKNOWLEDGMENTS

This work was supported by the National Science Foundation (NSF) through award OISE-1743701. The computational work was made possible through generous grants by the Texas Advanced Computing Center in Austin, TACC, Texas, and by the High Performance Computing facilities at UTA. H.A. acknowledges support by the Saudi Arabian Cultural Mission.

REFERENCES

(1) Zerr, A.; Miehe, G.; Serghiou, G.; Schwarz, M.; Kroke, E.; Riedel, R.; Fuess, H.; Kroll, P.; Boehler, R. Synthesis of Cubic Silicon Nitride. *Nature* **1999**, *400*, 340−342.

(2) Landskron, K.; Huppertz, H.; Senker, J.; Schnick, W. High-Pressure Synthesis of γ-P_3N_5 at 11 GPa and 1500 Degrees C in a Multianvil Assembly: A Binary Phosphorus(V) Nitride with a Three-Dimensional Network Structure from Pn4 Tetrahedra and Tetragonal PN_5 Pyramids. *Angew. Chem., Int. Ed.* **2001**, *40*, 2643−2645.

(3) Zerr, A.; Miehe, G.; Riedel, R. Synthesis of Cubic Zirconium and Hafnium Nitride Having Th_3P_4 Structure. *Nat. Mater.* **2003**, *2*, 185−189.

(4) Eremets, M. I.; Gavriliuk, A. G.; Trojan, I. A.; Dzivenko, D. A.; Boehler, R. Single-Bonded Cubic Form of Nitrogen. *Nat. Mater.* **2004**, *3*, 558−563.

(5) Gregoryanz, E.; Sanloup, C.; Somayazulu, M.; Badro, J.; Fiquet, G.; Mao, H. K.; Hemley, R. J. Synthesis and Characterization of a Binary Noble Metal Nitride. *Nat. Mater.* **2004**, *3*, 294−297.

(6) Zerr, A.; et al. High-Pressure Synthesis of Tantalum Nitride Having Orthorhombic U_2S_3 Type Structure. *Adv. Funct. Mater.* **2009**, *19*, 2282−2288.

(7) Bykov, M.; et al. Fe-N System at High Pressure Reveals a Compound Featuring Polymeric Nitrogen Chains. *Nat. Commun.* **2018**, *9*, No. 2756.

(8) Bykov, M.; et al. High-Pressure Synthesis of a Nitrogen-Rich Inclusion Compound ReN(8)xN(2) with Conjugated Polymeric Nitrogen Chains. *Angew. Chem., Int. Ed.* **2018**, *57*, 9048−9053.

(9) Laniel, D.; Dewaele, A.; Garbarino, G. High Pressure and High Temperature Synthesis of the Iron Pernitride FeN_2. *Inorg. Chem.* **2018**, *57*, 6245−6251.

(10) Laniel, D.; Weck, G.; Loubeyre, P. Direct Reaction of Nitrogen and Lithium up to 75 GPa: Synthesis of the Li_3N, LiN, LiN_2, and LiN_5 Compounds. *Inorg. Chem.* **2018**, *57*, 10685−10693.

(11) Zerr, A.; Riedel, R.; Sekine, T.; Lowther, J. E.; Ching, W. Y.; Tanaka, I. Recent Advances in New Hard High-Pressure Nitrides. *Adv. Mater.* **2006**, *18*, 2933−2948.

(12) Horvath-Bordon, E.; Riedel, R.; Zerr, A.; McMillan, P. F.; Auffermann, G.; Prots, Y.; Bronger, W.; Kniep, R.; Kroll, P. High-Pressure Chemistry of Nitride-Based Materials. *Chem. Soc. Rev.* **2006**, *35*, 987−1014.

(13) Salamat, A.; Hector, A. L.; Kroll, P.; McMillan, P. F. Nitrogen-Rich Transition Metal Nitrides. *Coord. Chem. Rev.* **2013**, *257*, 2063−2072.

DOI: 10.1021/acs.jpcc.9b00476
J. Phys. Chem. C 2019, 123, 7054−7060

(14) Mailhiot, C.; Yang, L. H.; Mcmahan, A. K. Polymeric Nitrogen. *Phys. Rev. B: Condens. Matter Mater. Phys.* **1992**, *46*, 14419−14435.
(15) Kroll, P. Hafnium Nitride with Thorium Phosphide Structure: Physical Properties and an Assessment of the Hf-N, Zr-N, and Ti-N Phase Diagrams at High Pressures and Temperatures. *Phys. Rev. Lett.* **2003**, *90*, No. 125501.
(16) Zhao, Z.; Bao, K.; Tian, F. B.; Duan, D. F.; Liu, B. B.; Cui, T. Phase Diagram, Mechanical Properties, and Electronic Structure of Nb-N Compounds under Pressure. *Phys. Chem. Chem. Phys.* **2015**, *17*, 22837−22845.
(17) Yu, S.; Zeng, Q. F.; Oganov, A. R.; Frapper, G.; Zhang, L. T. Phase Stability, Chemical Bonding and Mechanical Properties of Titanium Nitrides: A First-Principles Study. *Phys. Chem. Chem. Phys.* **2015**, *17*, 11763−11769.
(18) Liu, Z.; Li, D.; Wei, S. L.; Wang, W. J.; Tian, F. B.; Bao, K.; Duan, D. F.; Yu, H. Y.; Liu, B. B.; Cui, T. A. Bonding Properties of Aluminum Nitride at High Pressure. *Inorg. Chem.* **2017**, *56*, 7494−7500.
(19) Zhang, J.; Oganov, A. R.; Li, X. F.; Niu, H. Y. Pressure-Stabilized Hafnium Nitrides and Their Properties. *Phys. Rev. B: Condens. Matter Mater. Phys.* **2017**, *95*, 5.
(20) Sun, W. H.; Holder, A.; Orvananos, B.; Arca, E.; Zakutayev, A.; Lany, S.; Ceder, G. Thermodynamic Routes to Novel Metastable Nitrogen-Rich Nitrides. *Chem. Mater.* **2017**, *29*, 6936−6946.
(21) Huang, B. W.; Frapper, G. Barium-Nitrogen Phases under Pressure: Emergence of Structural Diversity and Nitrogen-Rich Compounds. *Chem. Mater.* **2018**, *30*, 7623−7636.
(22) Chase, M. W. *NIST-Janaf Thermochemical Tables*, NIST Standard Reference Database, 1998; 13. https://kinetics.nist.gov/janaf.
(23) Jacobsen, R. T.; Stewart, R. B.; Jahangiri, M. Thermodynamic Properties of Nitrogen from the Freezing Line to 2000-K at Pressures to 1000-MPa. *J. Phys. Chem. Ref. Data* **1986**, *15*, 735−909.
(24) Kroll, P.; Schroter, T.; Peters, M. Prediction of Novel Phases of Tantalum(V) Nitride and Tungsten(VI) Nitride That Can Be Synthesized under High Pressure and High Temperature. *Angew. Chem., Int. Ed.* **2005**, *44*, 4249−4254.
(25) Hohenberg, P.; Kohn, W. Inhomogeneous Electron Gas. *Phys. Rev.* **1964**, *136*, B864−B871.
(26) Kresse, G.; Hafner, J. *Ab Initio* Molecular Dynamics for Liquid Metals. *Phys. Rev. B: Condens. Matter Mater. Phys.* **1993**, *47*, 558−561.
(27) Kresse, G.; Hafner, J. *Ab Initio* Molecular-Dynamics Simulation of the Liquid-Metal/Amorphous-Semiconductor Transition in Germanium. *Phys. Rev. B: Condens. Matter Mater. Phys.* **1994**, *49*, 14251−14269.
(28) Kresse, G.; Furthmüller, J. Efficiency of Ab-Initio Total Energy Calculations for Metals and Semiconductors Using a Plane-Wave Basis Set. *Comput. Mater. Sci.* **1996**, *6*, 15−50.
(29) Sun, J.; Ruzsinszky, A.; Perdew, J. P. Strongly Constrained and Appropriately Normed Semilocal Density Functional. *Phys. Rev. Lett.* **2015**, *115*, No. 036402.
(30) Blöchl, P. E. Projector Augmented-Wave Method. *Phys. Rev. B: Condens. Matter Mater. Phys.* **1994**, *50*, 17953−17979.
(31) Kresse, G.; Joubert, D. From Ultrasoft Pseudopotentials to the Projector Augmented-Wave Method. *Phys. Rev. B: Condens. Matter Mater. Phys.* **1999**, *59*, 1758−1775.
(32) Perdew, J. P.; Burke, K.; Ernzerhof, M. Generalized Gradient Approximation Made Simple. *Phys. Rev. Lett.* **1996**, *77*, 3865−3868.
(33) Perdew, J. P.; Burke, K.; Ernzerhof, M. Generalized Gradient Approximation Made Simple [Phys. Rev. Lett. 77, 3865 (1996)]. *Phys. Rev. Lett.* **1997**, *78*, 1396.
(34) Unland, J.; Onderka, B.; Davydov, A.; Schmid-Fetzer, R. Thermodynamics and Phase Stability in the Ga-N System. *J. Cryst. Growth* **2003**, *256*, 33−51.
(35) Kroll, P. Assessment of the Hf-N, Zr-N and Ti-N Phase Diagrams at High Pressures and Temperatures: Balancing between MN and M_3N_4 (M = Hf, Zr, Ti). *J. Phys.: Condens. Matter* **2004**, *16*, S1235−S1244.
(36) Lipp, M. J.; Klepeis, J. P.; Baer, B. J.; Cynn, H.; Evans, W. J.; Iota, V.; Yoo, C. S. Transformation of Molecular Nitrogen to Nonmolecular Phases at Megabar Pressures by Direct Laser Heating. *Phys. Rev. B: Condens. Matter Mater. Phys.* **2007**, *76*, 2002.
(37) Gregoryanz, E.; Goncharov, A. F.; Sanloup, C.; Somayazulu, M.; Mao, H. K.; Hemley, R. J. High P-T Transformations of Nitrogen to 170 GPa. *J. Chem. Phys.* **2007**, *126*, No. 184505.
(38) Mattson, W. D.; Sanchez-Portal, D.; Chiesa, S.; Martin, R. M. Prediction of New Phases of Nitrogen at High Pressure from First-Principles Simulations. *Phys. Rev. Lett.* **2004**, *93*, No. 125501.
(39) Kroll, P.; von Appen, J. Post-Spinel Phases of Silicon Nitride. *Phys. Status Solidi B* **2001**, *226*, R6−R7.
(40) Weihrich, R.; Eyert, V.; Matar, S. F. Structure and Electronic Properties of New Model Dinitride Systems: A Density-Functional Study of CN_2, SiN_2, and GeN_2. *Chem. Phys. Lett.* **2003**, *373*, 636−641.
(41) Chen, C. B.; Xu, Y.; Sun, X. P.; Wang, S. H.; Tian, F. B. The Stability, Electronic Properties, and Hardness of SiN_2 under High Pressure. *RSC Adv.* **2014**, *4*, 55023−55027.
(42) Niwa, K.; Ogasawara, H.; Hasegawa, M. Pyrite Form of Group-14 Element Pernitrides Synthesized at High Pressure and High Temperature. *Dalton Trans.* **2017**, *46*, 9750−9754.
(43) Bhadram, V. S.; Kim, D. Y.; Strobel, T. A. High-Pressure Synthesis and Characterization of Incompressible Titanium Pernitride. *Chem. Mater.* **2016**, *28*, 1616−1620.
(44) Bhadram, V. S.; Liu, H. Y.; Xu, E. S.; Li, T. S.; Prakapenka, V. B.; Hrubiak, R.; Lany, S.; Strobel, T. A. Semiconducting Cubic Titanium Nitride in the Th_3P_4 Structure. *Phys. Rev. Mater.* **2018**, *2*, No. 011602.
(45) Kroll, P. Advances in Computation of Temperature-Pressure Phase Diagrams of High-Pressure Nitrides. *Key Eng. Mater.* **2008**, *403*, 77−80.
(46) Niwa, K.; Suzuki, K.; Muto, S.; Tatsumi, K.; Soda, K.; Kikegawa, T.; Hasegawa, M. Discovery of the Last Remaining Binary Platinum-Group Pernitride RuN_2. *Chem. - Eur. J.* **2014**, *20*, 13885−13888.
(47) Togo, A.; Kroll, P. First-Principles Lattice Dynamics Calculations of the Phase Boundary between β-Si_3N_4 and γ-Si_3N_4 at Elevated Temperatures and Pressures. *J. Comput. Chem.* **2008**, *29*, 2255−2259.
(48) Soignard, E.; McMillan, P. F. Raman Spectroscopy of γ-Si_3N_4 and γ-Ge_3N_4 Nitride Spinel Phases Formed at High Pressure and High Temperature: Evidence for Defect Formation in Nitride Spinels. *Chem. Mater.* **2004**, *16*, 3533−3542.
(49) Mosenfelder, J. L.; Von der Handt, A.; Furi, E.; Dalou, C.; Hervig, R. L.; Rossman, G. R.; Hirschmann, M. M. Nitrogen Incorporation in Silicates and Metals: Results from SIMS, EPMA, FTIR, and Laser-Extraction Mass Spectrometry. *Am. Mineral.* **2019**, *104*, 31−46.

DOI: 10.1021/acs.jpcc.9b00476
J. Phys. Chem. C 2019, 123, 7054−7060